

Size segregation of granular matter in silo discharges

Azadeh Samadani, A. Pradhan, and A. Kudrolli

Department of Physics, Clark University, Worcester, Massachusetts 01610

(Received 10 May 1999)

We present an experimental study of segregation of granular matter in a quasi-two-dimensional silo emptying out of an orifice. Size separation is observed when multisized particles are used with the larger particles found in the center of the silo in the region of fastest flow. We use imaging to study the flow inside the silo and quantitatively measure the concentration profiles of bidisperse beads as a function of position and time. The angle of the surface is given by the angle of repose of the particles, and the flow occurs in a few layers only near the top of this inclined surface. The flowing region becomes deeper near the center of the silo and is confined to a parabolic region centered at the orifice which is approximately described by the kinematic model. The experimental evidence suggests that the segregation occurs on the surface and not in the flow deep inside the silo where velocity gradients also are present. We report the time development of the concentrations of the bidisperse particles as a function of size ratios, flow rate, and the ratio of initial mixture. The qualitative aspects of the observed phenomena may be explained by a void filling model of segregation.

[S1063-651X(99)10912-7]

PACS number(s): 45.70.Mg, 81.05.Rm

I. INTRODUCTION

Segregation is often observed in granular matter subject to shear or external excitation. However, there have been very few studies where quantitative information on the development of segregation is available. The nature of segregation depends on many factors such as the geometry and the surface properties of the particles, velocity gradients, and boundary conditions [1–3]. For example in vibrated granular matter, segregation is observed, but the size concentration profiles depends on the shape of the container and the direction of the resulting convection [4–6]. In partially filled rotating cylinders, axial segregation depends on factors such as the filling fraction and rotation rates [7–9]. The absence of a satisfactory continuum theory to describe the macroscopic properties of granular matter and the complicated nature of the complex convection patterns which result under the above conditions makes the analysis of the segregation difficult.

In comparison, gravity driven flows offer an alternative for studying segregation where some progress has been made in understanding the flow [10,11]. One of the simplest types of flow is the slow flow of dense mixtures down an inclined surface. In this case free surface segregation has been studied using bidisperse particles [10]. Preferential void filling of small particles through the shear layer was identified as the main mechanism of segregation. This flow and the resulting surface segregation is similar to the situation where granular matter is poured into a silo [12]. In this case, the angle of repose quickly develops and the resulting flow is confined to a few layers at the surface. For polydisperse particles with similar surface properties, the larger particles are found at the bottom of the inclined surface and the smaller particles are found at the top. This segregation can be understood in the same way as the free surface segregation and can also be understood in terms of a capture model [13,14] based on work by Bouchaud *et al.* [15,16]. In the capture model the system is divided into flowing and static regions and the

smaller particles are assumed to be more easily captured by the static layer than the larger ones.

In this paper we consider flow in a silo which is filled uniformly with bidisperse particles and then drained from an orifice at the bottom. The nature of the flow is different because the flux of the particles is leaving the silo thus resulting in different boundary conditions. The resulting flow is more complex due to the development of a free surface and convergent flow near the orifice. Density waves are also known to occur [17].

To our knowledge, the only quantitative study of segregation in silo discharges is by Arteaga and Tuzun [18] who measured the volume ratio of a bidisperse mixture as a function of time, but did not visualize the internal flow. The ratio was found to be independent of time except at the very end of the discharge. It was speculated that the development of velocity gradients in the bulk due to the convergent flow is important for the observed segregation. The questions we address here are as follows. (1) Where does the segregation occur in the system? (2) What is the mechanism of segregation, that is, does it occur due to preferential void filling by small particles at the surface or is it due to the development of velocity gradients inside the silo? (3) What role does gravity play in segregation?

To address these questions, we used high resolution digital imaging to obtain detailed quantitative information on the evolution of particle segregation inside a quasi-two-dimensional silo. We find that there are static regions where there is no flow and mobile regions where the flow is very rapid. The latter region is parabolic in shape about the orifice. We observe that particles segregate so that the larger particles are found in the middle of the silo where the flow velocity is maximum. Although the large particles are found in the region with the maximum velocity, segregation actually occurs at the surface. The extent of segregation depends on the size ratio and the relative number of large and small particles in the initial mixture. This observed phenomena is consistent with the void filling model of segregation devel-

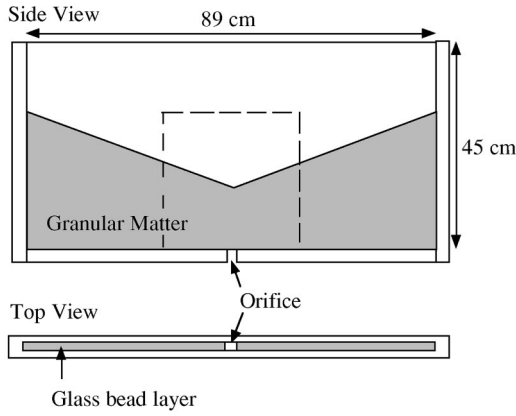


FIG. 1. Schematic diagram of the experimental apparatus. Grains pour out of an orifice at the bottom of a quasi-two-dimensional silo with a flow rate Q . The dashed box ($30\text{ cm} \times 30\text{ cm}$) indicates the area corresponding to images in Figs. 2 and 5.

oped in the context of flow down a rough inclined plane [10]. However, there are significant differences in the extent of segregation because of the details of the flow.

II. EXPERIMENTAL APPARATUS

Figure 1 shows the schematic diagram of the experimental setup. A rectangular silo of dimensions $89\text{ cm} \times 45\text{ cm}$ and a width w of 1.27 cm with an orifice at the bottom is used for the experiments. The surface and bulk flow inside the silo is visualized through the glass sidewalls of the silo using a 1000×1000 pixel noninterlaced Kodak ES 1.0 digital camera. A layer of 0.5 mm glass beads is glued to the bottom surface to obtain nonslip boundary conditions. The shape of the orifice is rectangular with dimensions $0.63\text{ cm} \times 1.27\text{ cm}$. A valve controls the flow rate through the orifice. The resulting flow is observed to be essentially two-dimensional. Limited experiments were also performed with a silo width of 2.54 cm to study the effect of the sidewalls on the flow.

We use glass beads with various sizes and shapes as listed in Table I [19]. The experiments are conducted in a controlled environment where the humidity is kept at 15% and the temperature is about 38°C . The data is insensitive to the temperature, but is sensitive to humidity above 25%.

III. OBSERVATIONS

We first discuss the data corresponding to 0.5 mm monodisperse glass beads (type M-1) to illustrate how the flow

TABLE I. Types of glass particles used in the experiments. The particles are approximately spherical and have a density $\rho = 2.42 \pm 0.05\text{ g/cm}^3$.

Type	Distribution	Size (mm)	Angle of repose, α
M-1	Monodisperse	0.5 ± 0.05	$24.5^\circ \pm 0.2^\circ$
M-2	Monodisperse	0.6 ± 0.05	$24.7^\circ \pm 0.2^\circ$
M-3	Monodisperse	0.7 ± 0.05	$24.5^\circ \pm 0.2^\circ$
M-4	Monodisperse	1.1 ± 0.10	$24.2^\circ \pm 0.2^\circ$
P-1	Polydisperse	$0.5 - 0.05$	$25.6^\circ \pm 0.2^\circ$
P-2	Polydisperse	$0.2 - 0.05$	$25.6^\circ \pm 0.2^\circ$

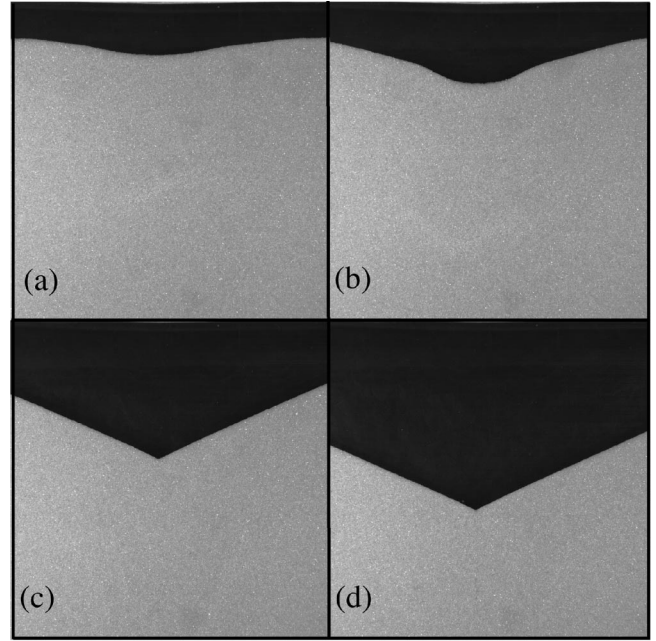


FIG. 2. Sequence of images of 0.5 mm monodisperse glass beads (type M-1) discharging ($Q = 15\text{ g/s}$) as a function of time: (a) $t = 10\text{ s}$; (b) $t = 20\text{ s}$; (c) $t = 100\text{ s}$; (d) $t = 200\text{ s}$.

develops as a function of time. A sequence of images of the glass beads as they discharge from the silo is shown in Fig. 2. The discharge rate $Q = 15\text{ g/s}$. The surface initially develops into an inverted Gaussian shape as shown in Fig. 2(b), and no rolling of grains is observed at the surface. Soon after, rolling occurs after the local slope exceeds the angle of repose α for the grains. At the same time the surface develops a V shape which is shown in Fig. 2(c). The angle the inclined surface makes with the horizontal equals the angle of repose and remains constant throughout the discharge, which takes approximately 500 s for this case. The length of the inclined surface increases linearly until the top of the surface reaches the side of the silo, and then remains constant.

A. Flow inside the silo

To identify the regions in motion, we subtract two images separated by a short time interval. Figure 3 shows the result of two images separated by 1.0 s . In the regions where the particles move, the intensities do not subtract to zero and give the speckled points in Fig. 3. Note that particles are completely stationary in the regions which are near the sides and a few layers from the surface. We divide the flowing phase into three regions as indicated in Fig. 3. The *surface flow* region, where the depth of the mobile layers increases roughly linearly down the incline. The *crossover* region, where the direction of the mean flow changes from along the surface to pointing toward the orifice. The *internal* region, where the convergent flow is very far from the surface. The interface between the moving and static regions [20] is plotted in Fig. 4 and is obtained by averaging over two nearest neighbors to average out fluctuations.

Flow near the orifice. The velocity distribution of the granular matter deep inside the silo has been described by a kinematic theory [11] based on a linear approximation for

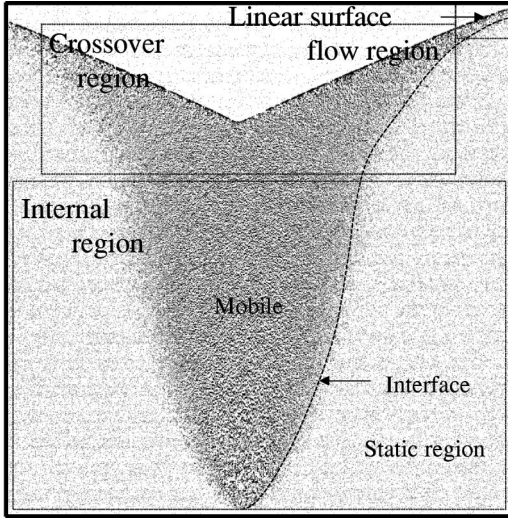


FIG. 3. Difference of images separated by time difference of 1 s. The regions which appear as gray are in motion ($Q=15$ g/s.) The regions in motion can be divided into the *surface flow* region, the *crossover* region, and the *internal* region.

the relation between the horizontal component of the velocity u and the gradient of the vertical velocity dv/dx , that is,

$$u = -B \frac{dv}{dx}, \quad (1)$$

where B is a constant which has dimensions of length. Combining Eq. (1) with the continuity equation yields an equation for the vertical component of the velocity v [11]:

$$\frac{\partial v}{\partial y} = B \frac{\partial^2 v}{\partial x^2}. \quad (2)$$

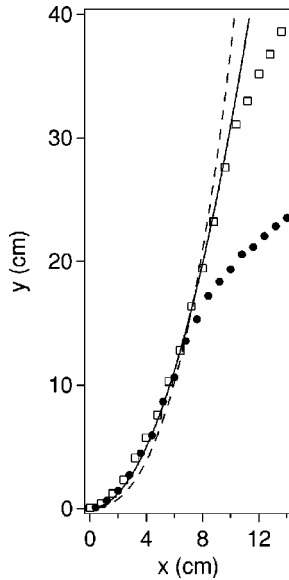


FIG. 4. The interface between the static and mobile regions at time $t=100$ s (\square) and $t=200$ s (\bullet). The interface actually corresponds to an equivelocity curve for which $v=0.03$ cm/s. Also shown is the comparison of the interface to a fit of the kinematic model [Eq. (4)] (dashed line) and a fit to a parabola (solid line). Note that far from the orifice the observed interface crosses over to a line which is parallel to the surface.

TABLE II. The width $a(v)$ [see Eq. (4)] of the parabolic fit that describes the interface of the deep flow near the orifice for different size beads and width w of the silo ($v=0.03$ cm/s.) The parameter B which relates the horizontal component of the velocity to the gradient of the vertical component in the kinematic model [see Eq. (4)] also describes the interface. The flow rate $Q=4.5$ g/s.

Type	$w=1.27$ cm $a(v)$ (cm)	$w=2.54$ cm $a(v)$ (cm)	$w=1.27$ cm B (cm)
M-4	0.20 ± 0.00	0.20 ± 0.00	0.38 ± 0.04
M-2	0.32 ± 0.01	0.36 ± 0.01	0.21 ± 0.02
P-1	0.40 ± 0.03	0.40 ± 0.03	0.18 ± 0.02
P-2	0.40 ± 0.03	-	-

The solution to Eq. (2) with appropriate boundary conditions in the converging flow regime is

$$v(x,y) = \frac{Q}{\rho \sqrt{4\pi B y}} e^{-x^2/4By}, \quad (3)$$

where x and y measure the horizontal and vertical position from the orifice, and ρ is the average mass density of particles relative to random close packing of the beads. Equation (3) can be rewritten to give the equivelocity contours

$$y = a(v)x^2 + 2Ba(v)y \ln y, \quad (4)$$

where $a(v) = 1/[4B \ln(v\sqrt{4B\rho}/Q)]$. The stream lines are also predicted by this theory and are given by

$$\psi = \frac{Q}{2\rho} \operatorname{erf}\left(\frac{x}{2\sqrt{4By}}\right). \quad (5)$$

Along the stream line ψ is a constant, and Eq. (5) gives

$$x = x_i \sqrt{By}, \quad (6)$$

where x_i is a constant that depends on the streamline.

Predictions similar to Eqs. (3) and (6) have been made using a diffusing void model [21,22]. In this model voids are assumed to diffuse from the orifice to the surface. Using a biased random walk model for the motion of the voids, the mean flow velocity can be estimated by calculating the frequency of a walker visiting a lattice site inside the silo.

We compare our data to the prediction of kinematic theory with B as a fitting parameter in Fig. 4. The theory is in reasonable agreement with the data, especially considering the simplicity of the model. However, as can be seen in Fig. 4, if we consider only the first term in Eq. (4), we obtain a better fit to the data. We summarize the results for the parameter, $a(v)$, and the kinematic model parameter, B , from fits to Eq. (4) in Table II. No significant dependence of the shape of the mobile region on the flow rate and the width of system was found, but B was found to depend on the size of the beads, which is consistent with the observations of Tuzun and Nedderman [23].

Flow near the surface. The description of flow using the kinematic model works only near the orifice. In the regions near the surface which are away from the sides, the flow is confined to a few layers. The number of layers increases

linearly down the inclined surface to about 10 layers. As the silo empties, the surface moves down, and the static layers begin to flow. The depth dependence of the velocity at the point where 10 layers are moving is approximately linear, that is,

$$v_s = v_0(1 - d/10) \text{ for } d < 10, \quad (7)$$

where v_0 is the average velocity of the particles at the surface, and d is the depth from the surface normalized by the mean particle size.

If all particles which leave the surface flow region eventually leave the silo from the orifice, then the velocity can be approximately related to the flux of material leaving the silo. Therefore the vertical and horizontal component of the velocity at the surface can be written as

$$v = \frac{Q}{10d\rho} \sin(\alpha) \text{ and } u = \frac{Q}{10d\rho} \cos(\alpha). \quad (8)$$

Therefore the velocity of the particles in the crossover regime changes from that given by Eq. (8) to that given by Eqs. (1) and (3). The direction of the mean flow changes from being parallel to the surface to pointing down towards the orifice. We note that convection rolls are not observed. The crossover region is approximately $15 \text{ cm} \times 15 \text{ cm}$ corresponding to hundreds of grains. We discuss in Sec. IV the details of the flow in the crossover regime and its effect on the observed segregation.

We note that the flow near the surface and around the obstacles has been also modeled by the diffusing void model [22]. This model gives a crossover which is very sharp and is of the order of one grain diameter. The scale over which the crossover occurs in our experiments is much broader as can be seen in Fig. 4.

B. Segregation

With this description of flow inside a discharging silo, we now report our experiments on bidisperse glass particles to study segregation. To visualize the segregation, two sizes of beads with different colors but identical surface properties are used. The symbol P_w is used to specify the percentage of larger particles by weight in the initial mixture in the silo. We first discuss the development of segregation when 1.2 mm yellow glass particles (M-4) are mixed with 0.6 mm blue glass particles (M-2) and therefore the diameter ratio is $r = 2$.

We pour the mixture ($P_w = 10\%$) into the silo as uniformly as possible. The development of the flow is similar to the monodisperse case described earlier, but we also observe that the density of the larger grains increases near the surface and the density of smaller grains increases in the moving layers below the surface. The evolution of segregation is shown in Fig. 5. In the case shown in Fig. 5, the particles were slightly segregated in layers during pouring to indicate the flowing region. Quantitative information was obtained with a more thoroughly mixed initial state.

To parametrize the segregation we measure the ratio of the two types of beads in a horizontal narrow rectangular region at a height of 5 cm above the orifice by measuring the light intensity. The light intensity is a monotonic function of

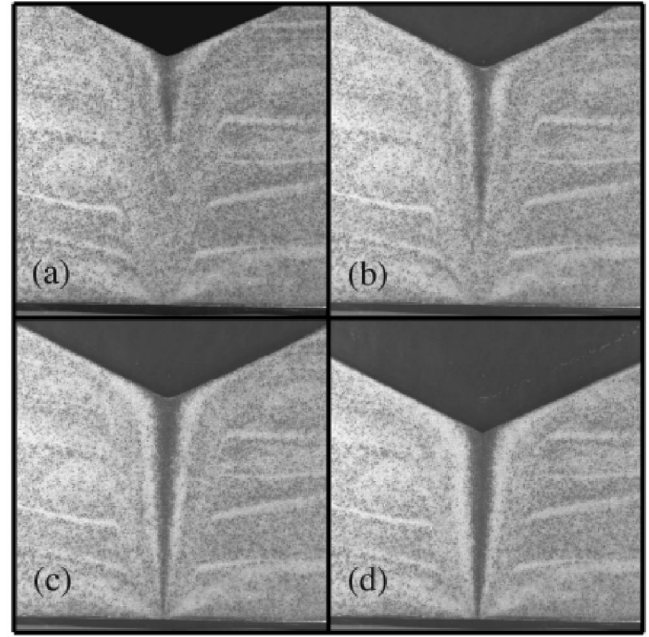


FIG. 5. Images of bidisperse particles inside the silo as a function of time ($r = 2.0$; $Q = 15 \text{ g/s}$.) The larger particles are found in the center of the flow.

the density ratio of the two kinds of particles. This function is determined by using known weight ratios of particles in a separate series of calibration experiments. The density ratio of the particles is plotted as a function of horizontal position and time in Fig. 6. We observe from Fig. 6 that the density of larger particles increases in the midpoint (directly above the orifice) as a function of time. The percentage of larger particles at the midpoint increases from 10%, corresponding to the initial mixture, to about 100%.

To further characterize the evolution of the segregation, we have plotted the density fraction of the large beads at the

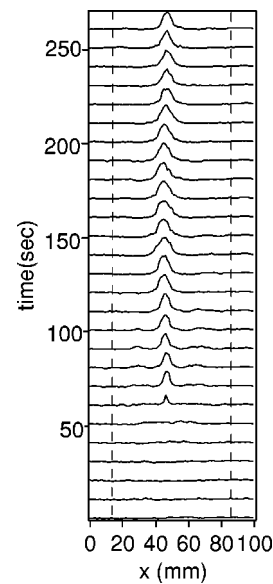


FIG. 6. The fraction of large particles as a function of time in a narrow region located at a height of 5 cm above the orifice. A peak develops at the center which grows higher and wider corresponding to the segregation of particles ($r = 2.0$, $P_w = 10\%$, $Q = 15 \text{ g/s}$). The dashed vertical lines indicate the mobile region.

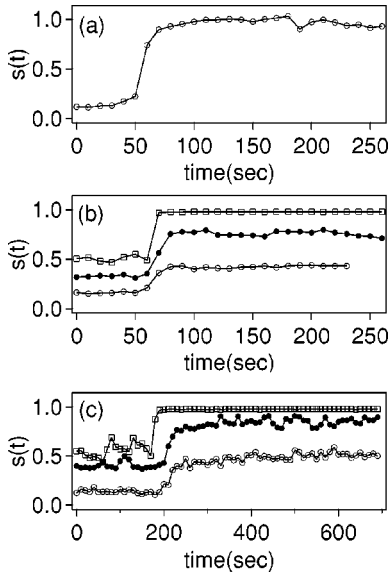


FIG. 7. (a) The segregation parameter $s(t)$ for $r=2$, and $P_W=10\%$, and $Q=15$ g/s. (b) The segregation for different initial values of P_W for $r=1.2$ [$P_W=15\%$ (\circ), $P_W=30\%$ (\bullet), and $P_W=50\%$ (\square)]. (c) Same as the data in (b) but at a lower flow rate ($Q=3.0$ g/s).

center point as a function of time [see Fig. 7(a)]. This density is called the “segregation parameter” $s(t)$. From Fig. 7(a) it can be seen that there is no segregation for the first 50 s after the start of the flow as can be also seen from Fig. 6. During this time we note that the velocity gradients of the grains in the silo are fully developed. The fact that $s(t)$ increases only after $t=50$ s indicates that the velocity gradients deep inside the silo are not responsible for segregation. We observe that a thin band of larger particles initially appears at the surface and grows down towards the orifice (see Fig. 5.) Because the observed area is near the bottom of the silo (5 cm above the orifice), it takes about 50 s for the larger particles to travel to the measured region for a flow rate of 15.0 g/s. After 50 s, $s(t)$ increases to about 1 and remains constant.

Effect of size ratio. We repeated the experiment with different size ratios to investigate the effect of different sizes on the segregation rates. For a mixture of 0.6 mm black glass beads (M-2) and 0.7 mm red glass beads (M-3) with $P_W=15\%$, the size ratio $r\approx 1.2$. Segregation is observed even for such a small size difference. A separate set of calibration curves for the density ratio of the particles was obtained in this case. The density distribution as a function of position and time with a flow rate of 15 g/s is similar to the larger size ratio, but the segregation does not occur as quickly and is less in comparison to the larger size ratio. As seen in Fig. 7(b), $s(t)\approx 0.15$ for $t\leq 50$ s, and then grows to about 0.3–0.35. Therefore $s(t)$ for $r=1.2$ is substantially smaller than for $r=2.0$.

For $r=1.2$, not only is the extent of segregation lower, but the interface between the region containing the large and small particles is more diffuse. The mass density ratio of the larger beads in the narrow rectangular region under observation is shown in Fig. 8 for $r=2.0$ and $r=1.2$. Both mass density ratios may be fitted by a Gaussian, with the Gaussian for higher r substantially narrower. In Sec. IV, we argue that the diffused nature of the interface between large and small

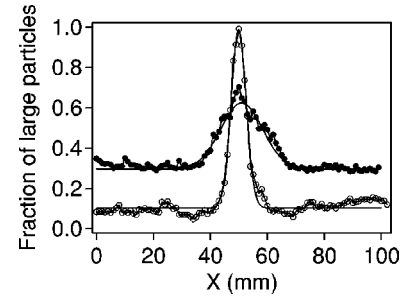


FIG. 8. The fraction of larger particles for $r=1.2$ (\bullet) and $r=2.0$ (\circ) as function of position at a height of 5 cm above the orifice at ($t=250$ s). The data is also fitted with a Gaussian to guide the eye. The region between large and small particles is more diffused for lower r .

particles for $r=1.2$ is a result of the nature of the flow in the crossover region.

It can be also seen from Fig. 7 that the saturation point of the segregation parameter $s(t)$ depends on the diameter ratio r and the density ratio P_W . If the segregation is not complete, there are fluctuations in the number ratio of the particles about the saturation value. The fluctuations are stronger when the saturation is lower.

Experiments were also performed with polydisperse particles (P-1 and P-2 in Table I), and segregation was also observed with larger particles found at the center as in the bidisperse cases already discussed. No quantitative data was obtained for polydisperse particles.

Effect of number ratio of large and small particles. We considered the effect of smaller values of the density ratio P_W on the extent of segregation by doing experiments with $P_W=30\%$ and 50% . The results of these experiments also are plotted in Fig. 7(b). The overall development of segregation is similar, but the extent depends on P_W . From Fig. 7(b), we observe that the saturation level of segregation increases for higher P_W . The saturation value is found to fluctuate on the order of 5%.

Effect of flow rate. We repeated all the experiments with a flow rate of 3.0 ± 0.5 g/s, which corresponds to the slowest rate for which continuous flow is possible in our system. The behavior of the segregation parameter $s(t)$ is similar to the faster flow rate of 15 g/s and is shown in Fig. 7(c). For the slower flow rate, no segregation occurs for $t<200$ s. This time is longer because the segregated particles at the surface take a longer time to arrive in the region where we monitor $s(t)$. The ratio of times for the development of the segregation is approximately the same as the ratio of the flow rates. There are small changes in the value of $s(t)$, but these changes are the same order as the errors in the calibration of the density ratio.

IV. DISCUSSION

Because the data clearly suggests that segregation occurs at the surface (see Fig. 9), we first explore the relevance of a model proposed by Savage and Lun [10] based on their experiments on simple flows on an inclined plane. They considered a shear flow of a thin layer of bidisperse glass beads down a rough inclined plane and obtained quantitative data for the development of segregation. The beads were col-

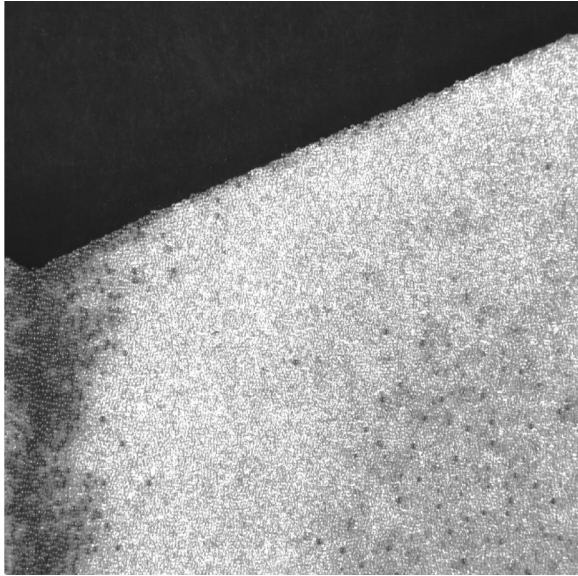


FIG. 9. An image of segregated particles. The larger particles (black) are rolling on top of layers of small particles (white) ($r = 2$).

lected from different heights in the layer using an arrangement of baffles which directed the beads into different bins [10]. They considered two mechanisms to explain the development of segregation: (i) the preferential filling of voids in a lower layer by smaller particles, and (ii) the expulsion of particles to the top layer (which is not size dependent) to make the net flux through a layer zero.

The probability of interlayer percolation of particles is calculated by considering the relative probabilities of small and large particles falling into possible voids as a function of the size and the number ratio of the two types of particles (see Fig. 10). The resulting probability is an exponential function of particle sizes and average void size [10]. Therefore, the probability for small particles to fall into voids is significantly higher than that for larger particles if the voids created are of a similar size. By then assuming a linear profile for the velocity as a function of depth in the layer and a constant velocity along the inclined plane, they were able to calculate relations for the concentration profiles of the particles as a function of depth in the layer and position down the inclined plane. Their model predicts that the particles segregate completely after traveling a certain distance down the incline which depends on the size ratio and volume density ratio of the initial mixture, and the angle of inclination of the plane.

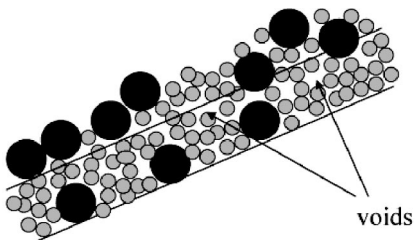


FIG. 10. The void filling mechanism at the surface appears to be responsible for the observed segregation. Smaller particles have a higher probability to fill a void compared to larger particles for a comparable sized void.

In our experiments in silo discharges, the flow in the surface flow region (see Fig. 3) is similar to that considered by Savage and Lun [10]. Therefore, we can qualitatively explain the observed segregation of particles inside the silo by the mechanism of preferential filling of voids by smaller particles near the surface. Particles are then carried along the streamlines which results in the larger particles being in the central region of the silo where the flow velocity is highest (also see Fig. 9). However, a quantitative comparison with the predictions of Ref. [10] cannot be done because of significant differences in the underlying flow. In our experiments, the flux of particles comes from the static layers being converted to mobile layers, whereas in the simple inclined flow, the particles enter at one point at the top of the inclined plane. In addition, the flow near the bottom of the surface acquires a significant vertical component.

We also find that the inclined surface grows linearly as the silo discharges until the surface reaches the edge of the silo and then remains constant. If the segregation depends on the length of the surface as calculated in Ref. [10], then we would expect $s(t)$ to increase during the time the surface length increases. In our experiments, $s(t)$ saturates to values less than 100% for small r over a range of values of P_W during a time which is less than the time for which the surface length increases. The complications introduced by the additional features in the flow have to be taken into account to explain saturation of less than 100% in $s(t)$ for small r .

One possible explanation for the saturation is as follows. In addition to voids being created due to fluctuations in the interlayer velocity, the vertical component of the velocity becomes significant in the crossover regime. Thus particles create larger voids behind them in the crossover regime (see Fig. 3) in comparison to the surface flow regime. Therefore, the probability of finding larger voids where large particles can fall into increases in the crossover regime. At some point on the inclined surface, the difference between the probability of a void being filled by a small or large particle becomes negligible. This point might be expected to occur higher on the inclined plane for smaller size differences resulting in lower saturation values for $s(t)$.

This saturation appears to occur for $r = 1.2$ as seen in Fig. 8. If the size ratio r is large enough, the probability for smaller particles to fill a void remains much higher and complete segregation is seen for $r = 2$ in Fig. 8.

It might be expected that the change in flow rate would affect segregation because the creation of voids depends on the fluctuations and value of the mean velocity. Because the void filling mechanism is important for segregation, the quantitative progress of segregation may depend on the size ratio and flow rate. However, these changes appear to be not important in the range of flow rate available in our experiments.

The data for $t < 50$ s and $Q = 15$ g/s in Fig. 7 also shows that the void filling mechanism is unimportant if the direction of flow is in the same direction as the gravitational field as is the case in the deep flow regime of the silo. Segregation of bidisperse particles in the absence of a gravitational field has been considered in a ‘‘collisional’’ flow by Jenkins [24]. The difference in the scattering rates for the two different size particles is anticipated to give rise to segregation for

rapid flow. However, the velocities of the particles in the silo may be too small for such effects to be important.

V. SUMMARY

In summary, we have reported experiments on segregation of bimixtures of glass beads in a discharging silo. Using digital imaging we characterized the flow and measured the development of segregation as a function of position and time. The flow deep inside the silo is approximately characterized by the kinematic model [11], but more theoretical developments are required to model the flow near the surface. Segregation is observed even for very small size ratios. We observe that segregation occurs at the surface and not in the bulk where velocity gradients are also present. We quantitatively characterize the development and progress of the segregation using the mass ratio $s(t)$. We also obtained quantitative information about the size distribution of the particles inside the silo (see Fig. 8 for example). Our experiments also indicate that the segregation progresses very

quickly if the surface flow is not along the direction of the gravitational field.

A qualitative explanation of the distribution of concentration of large and small particles can be given by using the void filling mechanism. However, a quantitative explanation requires a better understanding of the velocity profiles near the surface and its role on creating voids which drive flow and segregation. Quantitative experimental data for the spatial and time development of segregation is scarce, and the data presented in this paper provides a guide to the development of models of segregation.

ACKNOWLEDGMENTS

We thank D. Hong, L. Mahadevan, and H. Gould for useful discussions, and J. Norton for technical assistance. This work was partially supported by the Donors of the Petroleum Research Fund administered by the American Chemical Society and one of us (A.K.) was also funded by the Alfred P. Sloan Foundation.

-
- [1] D. J. Stephens and J. Bridgewater, *Powder Technol.* **21**, 29 (1978).
 - [2] J. Bridgewater, in *Granular Matter*, edited by A. Mehta, (Springer-Verlag, Berlin, 1993), p. 161.
 - [3] H. M. Jaeger, S. R. Nagel, and R. P. Behringer, *Phys. Today* **49** (4), 32 (1996); *Rev. Mod. Phys.* **68**, 1259 (1996).
 - [4] A. Rosato, K. J. Strandburg, F. Prinz, and R. H. Swendsen, *Phys. Rev. Lett.* **58**, 1038 (1987).
 - [5] J. B. Knight *et al.*, *Phys. Rev. E* **54**, 5726 (1996).
 - [6] J. B. Knight, *Phys. Rev. E* **55**, 6016 (1997).
 - [7] O. Zik *et al.*, *Phys. Rev. Lett.* **73**, 644 (1994).
 - [8] K. Hill and J. Kakalios, *Phys. Rev. E* **52**, 4393 (1995).
 - [9] D. V. Khakhar, J. J. McCarthy, T. Shinbrot, and J. M. Ottino, *Phys. Fluids* **9**, 31 (1997).
 - [10] S. B. Savage and C. K. K. Lun, *J. Fluid Mech.* **189**, 311 (1988).
 - [11] R. M. Nedderman and U. Tuzun, *Powder Technol.* **22**, 243 (1979).
 - [12] P. Cizeau, H. Makse, and H. E. Stanley, *Phys. Rev. E* **59**, 4408 (1999).
 - [13] T. Boutreux and P. G. de Gennes, *J. Phys. I* **6**, 1295 (1996).
 - [14] T. Boutreux, *Eur. Phys. J. B* **6**, 419 (1998).
 - [15] J.-P. Bouchaud, M. E. Cates, J. R. Prakash, and S. F. Edwards, *J. Phys. I* **4**, 1383 (1994).
 - [16] J. -P. Bouchaud, M. E. Cates, J. R. Prakash, and S. F. Edwards, *Phys. Rev. Lett.* **74**, 1982 (1995).
 - [17] G. W. Baxter, R. P. Behringer, T. Fagert, and G. A. Johnson, *Phys. Rev. Lett.* **62**, 2825 (1989).
 - [18] P. Arteaga and U. Tuzun, *Chem. Eng. Sci.* **45**, 205 (1990); U. Tuzun and P. Arteaga, *ibid.* **47**, 1619 (1992).
 - [19] The glass beads were obtained from Jaygo Incorporated, New Jersey.
 - [20] This interface corresponds to an equivelocity contour for a very small magnitude of velocity which is of the order of the size of a pixel divided by the time difference between the two images used in identifying the moving regions.
 - [21] W. W. Mullins, *Powder Technol.* **9**, 29 (1974).
 - [22] H. Caram and D. C. Hong, *Phys. Rev. Lett.* **67**, 828 (1991); *Mod. Phys. Lett. B* **6**, 761 (1992).
 - [23] U. Tuzun and R. M. Nedderman, *Powder Technol.* **24**, 257 (1979).
 - [24] J. T. Jenkins, *Physics of Dry Granular Media* (Kluwer, Dordrecht, 1998), p. 645.